JTTEE5 15:670-675
DOI: 10.1361/105996306X147090
1059-9630/$19.00 © ASM International

Peer Reviewed

A New High-Velocity Oxygen Fuel Process for Making Finely Structured and Highly Bonded Inconel Alloy Layers from Liquid Feedstock

X.Q. Ma, J. Roth, D.W. Gandy, and G.J. Frederick

(Submitted February 20, 2006; in revised form June 6, 2006)

High-velocity oxygen fuel (HVOF) thermal spray processes are used in applications requiring the highest density and adhesion strength, which are not achievable in most other thermal spray processes. Similar to other thermal spray processes, however, a normal HVOF process is unable to apply fine powders less than 10 μm via a powder feeder. The advantages of using smaller and even nanosized particles in a HVOF process include uniform microstructure, higher cohesion and adhesion, full density, lower internal stress, and higher deposition efficiency. In this work, a new process has been developed for HVOF forming of fine-grained Inconel 625 alloy layers using a liquid feedstock containing small alloy particles. Process investigations have shown the benefits of making single and duplex layered coatings with full density and high bond strength, which are attributed to the very high kinetic energy of particles striking on the substrates and the better melting of the small particles.

Keywords bond strength, high-velocity oxyfuel, Inconel alloy coating, microstructure, liquid feedstock, suspension, process diagnostic.

1. Introduction

In a steam-electric fossil-fuel-fired plant, one of the severe problems is the failure of water boiler walls, piping components, and supports (Ref 1). The lifetime of the boiler components is limited by high pressures and thermal loads as well as gradual wall thinning induced by high-temperature oxidation, hot corrosion, sulfidation, erosion, and overheating, especially on fire/ash side (Ref 2-4). Surface modification and coating techniques have proven to be effective methods to reduce the degradation and damages, and prevent the boiler walls/pipes from unpredicted failures.

Many coating techniques and coating systems have been developed and used for preventing the deterioration of the underlying steel tubes, such as T2, T11, and T22. Of various types of coatings and processes, commercially available protective systems include weld overlay deposits, thermal spray coatings, and chromized and aluminized coatings. The weld overlay method is capable of applying thick layered coatings with a high efficiency, as well as on-site welding and repair capabilities. However, this type of coating presents problems of microsegregation and preferential corrosion, susceptibility of circumferential cracking, induced residual stress, tube warping, and formation of brittle fusion line interface (Ref 5-7). Thermal spray techniques, including arc spray, plasma spray, high-velocity oxygen fuel (HVOF) spray, and detonation spray, have been extensively used for producing various types of stainless steels, alloys, intermetallic compounds, and carbide cermet coatings onto the surfaces of boiler walls/tubes. Thermal sprayed coatings have the advantages of flexibility in coating materials and processes and also of minimizing heat-affected zones in the workpieces. Drawbacks of thermal sprayed coatings include defective microstructure and the lack of metallurgical bonding to the substrate. Consequently, these coatings are susceptible to property degradation and exhibit a high risk of flaking after exposure to corrosion, oxidation, and erosion attack under thermal shock condition (Ref 8-10).

Among thermal spray techniques, HVOF (also detonation process) provides the highest coating-to-substrate bond strength and highest coating density and thus is proven to be more acceptable for boiler applications. However, the low degree of powder melting in HVOF caused by relatively low flame temperature and short particle resident time in the flame has limited further improvement in coating quality. More desirable properties of HVOF coatings can only be obtained by treating the coatings in supplementary processes. One method is laser melting (Ref 11, 12), which has the disadvantages of additional costs and thermal stress-induced coating damages. An alternative way for increasing the melting in HVOF coatings is to use smaller powder feedstocks. However, fine powder feedstocks are very difficult to supply at a constant feed rate when their size is below 10 μm. In this work, the authors report an innovative

This article was originally published in *Building on 100 Years of Success, Proceedings of the 2006 International Thermal Spray Conference* (Seattle, WA), May 15-18, 2006, B.R. Marple, M.M. Hyland, Y.-Ch. Lau, R.S. Lima, and J. Voyer, Ed., ASM International, Materials Park, OH, 2006.

X.Q. Ma and **J. Roth,** Inframat Corporation, Farmington, CT; and **D.W. Gandy** and **G.J. Frederick,** Electric Power Research Institute, Charlotte, NC. Contact e-mail: xma@inframat.com.

Table 1 Composition and size distribution of coating materials

Materials	Composition, wt.%	Size, μm
Inconel 625	Ni-21.4Cr-8.9Mo-3.57(Nb + Ta)-0.06Al-0.05Co-0.26Fe-0.05Ti-0.023Si-0.06C	+20−52
Fine Inconel 625	Ni-21.4Cr-8.9Mo-3.57(Nb + Ta)-0.06Al-0.05Co-0.26Fe-0.05Ti-0.023Si-0.06C	<11
Self-flux alloy	Ni-14.55Cr-3.22B-4.7Si-4.78Fe	+16−42

HVOF process using a particle/liquid slurry feedstock where fine particles are suspended in a liquid media to form a fine particle/liquid suspension followed by injection of the slurry feedstock into a HVOF flame. The liquid not only acts as a particle carrier, but also, in the case of an organic liquid, adds an exothermal effect to the flame for enhanced particle melting. Based on the microstructures and coating properties, finely structured coatings were obtained in this newly developed slurry feeding HVOF process. This process has demonstrated a high degree of particle melting and coating-to-substrate bonding.

2. Experimental Details

2.1 Substrate Materials

An AISI 1018 carbon steel was used as the substrate in this study. The specimens have a dimension of 100 × 100 × 3 mm^3 for process trials, 60 × 60 × 0.75 mm^3 for mechanical property tests, 25.4 mm in diameter and 2 mm in thickness for thermal cycling test, and 25.4 mm in diameter for ASTM standard tensile tests. Type 316 stainless steel disks of 25.4 mm in diameter and 3 mm in thickness were also used for thermal cycling tests.

2.2 Coating Materials and Chemicals

The powders used for the coatings are listed in Table 1. Other materials including iron-chromium (Fe-Cr) alloy were also studied, but are reported elsewhere. Reagent-graded chemicals were used to form the liquid suspension. One feedstock was water based with surfactant additives (feedstock No. 1), and other was organic based with additives (feedstock No. 2).

2.3 Liquid Suspension HVOF Spray (LS-HVOF)

A Diamond Jet 2700 hybrid HVOF spray system (Sulzer-Metco, NY) equipped with a turntable, six-axis robot and a liquid delivery device was used to spray the liquid feedstock. The fuel used was propylene, and routine surface preparation procedures were applied prior to the HVOF spraying. Thermal spray parameters were optimized based on microstructural analyses and process diagnostic methods. In LS-HVOF as shown in Fig. 1, the fine alloy powder was well mixed with the liquid (water or organic). The liquid slurry feedstock was pumped to a liquid port and coaxially fed into the HVOF gun via a modified liquid feeding injector. Flow of the liquid suspension was typically controlled at a rate of 120 to 160 mL/min (20 to 30 g/min). SprayWatch diagnostics system (Model-2i, OSeir, Finland) was set up to determine particle temperature and velocity. The types of the

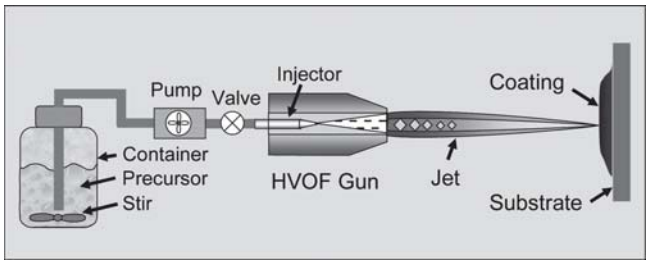

Fig. 1 Liquid precursor high-velocity oxygen fuel spray process (LS-HVOF)

Table 2 Sprayed coatings made by HVOF or LS-HVOF processes

Code	Materials	Coating structure	Process
No. 1	Inconel 625	Single layer ~250 μm	HVOF
No. 2	Self-flux + alloy 625	Primer (~40 μm) + Topcoat (~250 μm)	HVOF
No. 3	Inconel 625 (Precursor No. 1)	Single layer ~250 μm	LS-HVOF
No. 4	Self-flux (HVOF) + alloy 625 (Precursor No. 1)	Primer (~40 μm) + Topcoat (~250 μm)	LS-HVOF
No. 5	Inconel 625 (Precursor No. 2)	Single layer ~250 μm	LS-HVOF

HVOF and LS-HVOF coatings are listed in Table 2. The HOVF coating No. 1 and LS-HVOF coatings No. 2 to 5 were produced at a spray distance of 250 and 300 mm, respectively. A spray distance of self-flux alloy (40 to 100 μm) was sprayed as a primer layer and Inconel alloy 625 as a topcoat in the duplex coatings.

2.4 Characterization and Evaluation of Coatings

2.4.1 Microstructure. Coating microstructures were evaluated using a metallographic procedure, mainly on the cross sections under optical and scanning electron microscopes. Coating porosity, unmelted particles, and coating-to-substrate interfaces were examined. Fractured morphologies of the coatings were observed to determine the degree of particle melting in the coatings.

2.4.2 Mechanical Test. Tensile bond strength tests were performed according to ASTM C 633 standard (Ref 13). The tensile buttons were joined using a metallic brazing method. In addition to tensile pull test, a nonstandard ball punch deformation test was used to evaluate coating ductility and adhesion. In the punch test, a steel ball penetrator was placed on the substrate side against a cylindrical die. When a load was applied to the punch ball at a constant displacement rate, the substrate and the coating experienced a deformation. The deformed coatings were examined qualitatively in terms of damage severity and pattern.

2.4.3 Adhesive Test in Thermal Cycling. One thermal cycle consisted of 10 min heating at 800 °C in a tube furnace and 10 min forced-air cooling to room temperature out of the furnace. The tested coatings were sprayed on 1 in. diameter steel and stainless steel substrates. The lifetime referred to the accumulated cycle number per time upon the occurrence of coating spallation at 20% total coating area.

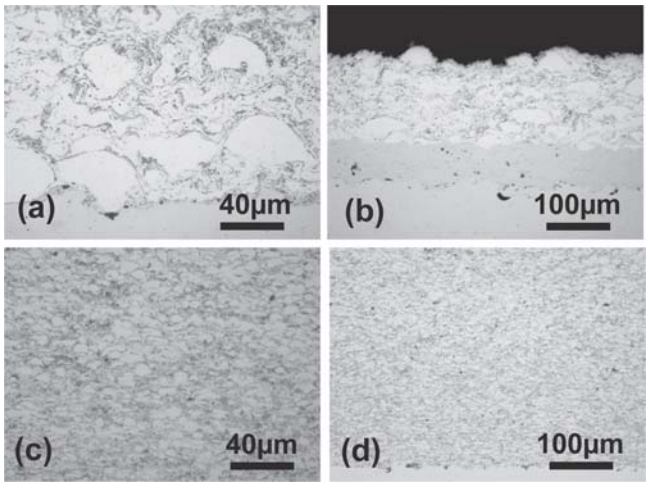

Fig. 2 Cross-sectional micrographs of Inconel 625 coatings made by (a) HVOF process No. 1, (b) HVOF process No. 2, which has a self-flux alloy primer, (c) LS-HVOF process No. 3 with fine particles, and (d) LS-HVOF process No. 4 with a primer

2.4.4 Erosion Test. In a grit-blasting chamber, 1 in. diameter disk sample was mounted in a sample holder, then a propane-oxygen torch was used to heat the sample from the substrate side. A blasting nozzle was positioned normal to the coating surface (90°) at a distance of 125 mm and operated under a pressure of 35 psi and a flow rate of 115 g/min using an alumina grit (mesh 30). The tests were performed at 25 and 300 °C, respectively. Erosion rate was determined based on the average volume loss of three identical samples per coating, blasting time, and surface area for each sample.

3. Results and Discussion

3.1 Microstructure

Typical cross-section micrographs of the sprayed coatings are shown in Fig. 2. As could be expected, a conventional HVOF sprayed Inconel 625 coating is quite dense, well adhered, and less oxidized, but has many inclusions of unmelted or partially melted particles (Fig. 2a). Self-flux alloy primer indicates a nearly full density due to its relative low melting point and perfectly clean and bonded interface with the substrate and the topcoat (Fig. 2b). In Fig. 2(c) and (d), it is obvious that the Inconel alloy 625 layers formed via the newly developed LS-HVOF process have much finer splats compared with those formed in a normal HVOF process. This is attributed to the use of the small feeding powders.

The degree of particle melting was evaluated by observing the fractured coating morphologies. In HVOF-formed Inconel 625 coatings, there are many spherical particles (>20 μm), indicating a low degree of feedstock melting. The area percentage of the unmelted spheres to the well-melted splats is at least 40%, as seen in Fig. 3(a). In contrast, the LS-HVOF coatings contain much fewer spherical inclusions as shown in Fig. 3(b), indicating a higher degree of feedstock melting. This observation is consistent with the cross-sectional microstructural views and the coating surface roughness measurements. The LS-HVOF alloy

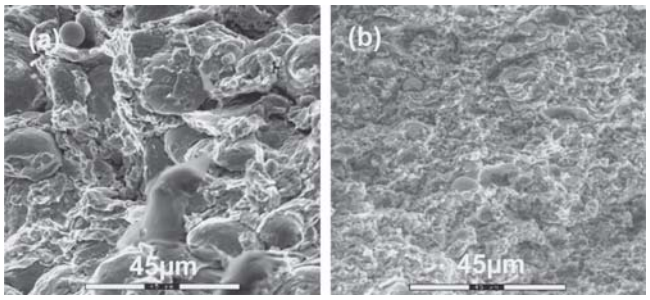

Fig. 3 Fractured morphologies of the coatings formed in (a) HVOF process No. 1, with many unmelted inclusions and (b) LS-HVOF process No. 3, showing a much finer splatted microstructure

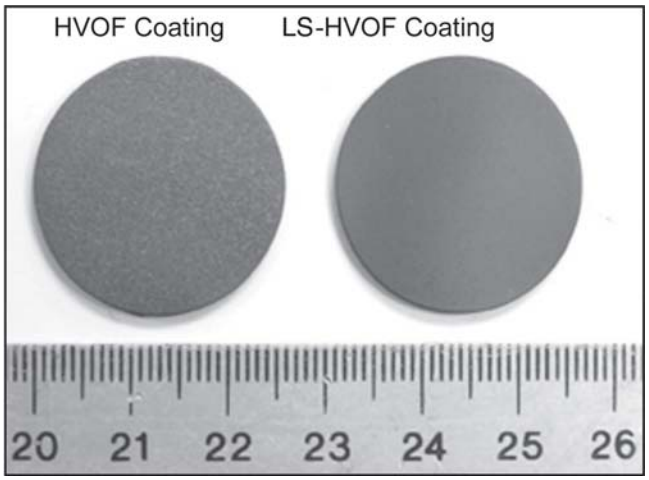

Fig. 4 Optical surface graphs of the specimens produced by HVOF process No. 1 (left) and LS-HVOF process No. 3 (right)

coatings are much smoother, with an average roughness (R_a) of 2.5 μm, than those conventional HVOF coatings, with a R_a of 8.3 μm as shown in Fig. 4.

3.2 Process Diagnostic Analysis

Process diagnostics were performed for both HVOF and LS-HVOF processes to determine the optimized process parameters and to understand the difference between these two processes. Two important parameters, particle temperature and velocity, were measured at different spray distances.

Typical profiles of particle temperature and velocity distribution along the radial direction of flame are shown in Fig. 5 for a LS-HVOF process. The central temperature and velocity are about 2020 °C and 600 m/s, respectively. Figure 6 presents the measured temperature and velocity for three processes at several spray distances ranging from 200 to 350 mm. In general, at a short spray distance of 200 mm, LS-HVOF process No. 5 provides the highest velocity from 600 to 700 m/s, and a particle temperature similar to or slightly higher than those of normal HVOF processes. The LS-HVOF process No. 3 shows a slightly higher velocity but much lower temperature relative to the conventional HVOF process. Inversely, at a further spray distance, the HVOF process shows a higher temperature and velocity than

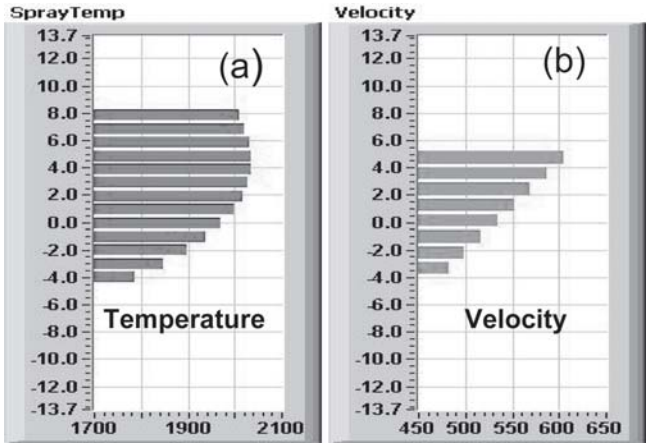

Fig. 5 Typically radial distribution profiles of (a) particle temperature and (b) velocity in LS-HVOF process No. 5, in which an organic precursor was used for exothermal effect

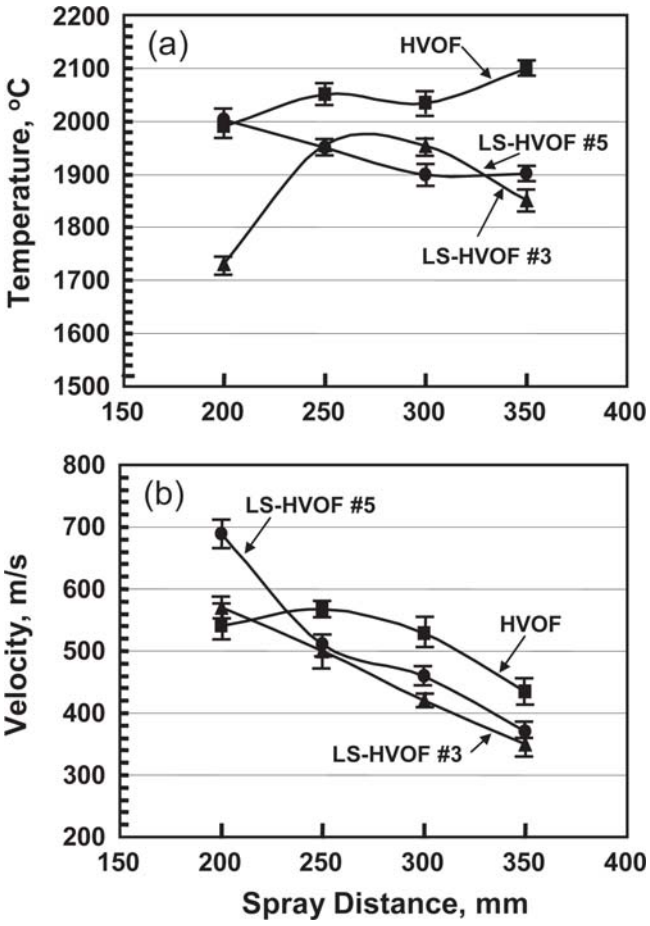

Fig. 6 The dependency of (a) temperature and (b) velocity on spray distances for HVOF and LS-HVOF processes

the LS-HVOF process. The changes of the two parameters (particle temperature and velocity) versus spray distance are directly related to the heating history of powders having different particle sizes.

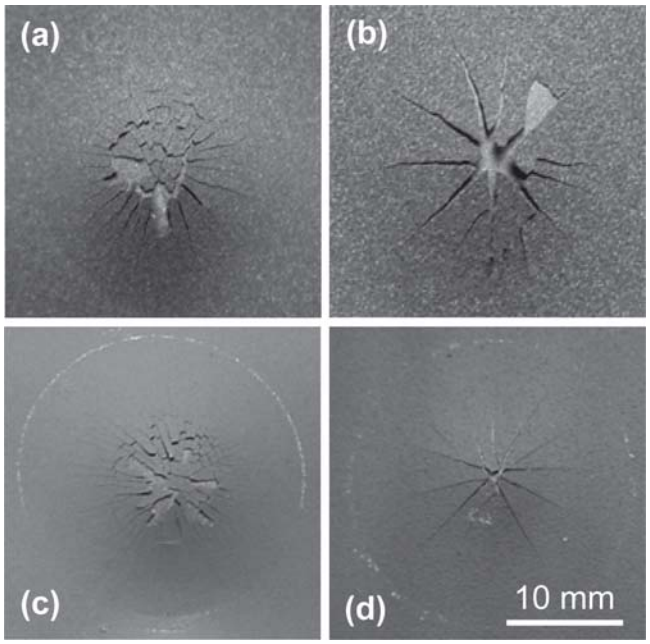

Fig. 7 Top views of the specimens tested in ball punch tests. (a) HVOF formed Inconel 625 coating. (b) HVOF-625 coating with a self-flux alloy primer. (c) LS-HVOF No. 3 formed alloy 625 coating. (d) LS-HVOF No. 3 formed Inconel 625 coating with a self-flux alloy primer

The coarse particles used in the HVOF process need longer traveling distance and resident time in the flame to be melted and accelerated. In LS-HVOF process No. 5, an organic-based suspension was used that added exothermal heat to the flame. In LS-HVOF process No. 3, water-base suspension took some heat from the jet during water evaporation and resulted in a relatively lower particle temperature, especially at a short spray distance. Although there was not a dramatic increase in particle temperature or velocity in the LS-HVOF processes, the capability for feeding finer particles into the HVOF jet could greatly promote powder melting and coating integrity, including high cohesion and adhesion properties. It is worthwhile to point out that particles in the size range of several microns could theoretically be melted completely, but their temperature could not be recorded because of the limited detection sensitivity of the camera. The actual particle temperature for most of fine particles should be much higher than the recorded average temperature. This assumption is consistent with the observations on the fractured surfaces that indicate a high degree of melting in the LS-HVOF coatings.

3.3 Mechanical Properties

Ball punch test is widely used for evaluating the ductility of metallic sheet materials. In this study, this test was performed to evaluate the ductility and the adhesion of the sprayed coatings based on visual observations of fracture and delamination patterns on the tested samples. Figure 7 shows the top view of the tested coatings. For coatings without a self-flux bond coat (Fig. 7a and c), they all exhibited severe cracking and local peeling. The LS-HVOF coating had a slightly smaller spallation area and short crack length, but a higher cracking density relative to the

Table 3 Erosion rates of the coating specimens tested at room temperature and 300 °C

	Erosion rate, $\times 10^{-2}$ mm^3 · min	
Coatings	**25 °C**	**300 °C**
HVOF No. 1	3.012	3.384
LS-HVOF No. 3	7.62	9.12
LS-HVOF No. 5	9.72	7.32

HVOF coating. Assuming that there was no significant improvement in the ductility of LS-HVOF coatings, the different cracking density may be attributed to the difference in terms of deformation energy release, that is, the form of cracking with a good bonding in LS-HVOF coating and of debonding with less cracking in HVOF coating, respectively.

The coatings with a self-flux alloy primer showed quite different fracture morphologies compared with the coatings without a primer. Cracks propagated radially from the top of the punching points, and the number of cracks is much less (Fig. 7b and d) for the coatings with a primer. The use of self-flux alloy bond coat to improve coating adhesion has been well studied (Ref 14-16), and it seems true for the HVOF coating and the LS-HVOF coating in this work. Tensile tests were conducted to verify the bonding improvement; unfortunately, results were inconsistent mostly due to uneven brazing of the tensile buttons. These initial results indicated it would be worthwhile to attempt a much finer particle size (several microns or submicron sizes) for a higher coating ductility and adhesion in future work.

3.4 Coating Adhesion in Thermal Cycling Test

Thermal cycling test has accumulated a total 10,080 cycles so far, and no peeling or spalling has occurred on the tested coatings, with the exception of HVOF coating (No. 2) that failed at 7950 cycles with a detached area of about 20% of the total coating area. The detachment was initiated from the edge of the disk and existed at the coating to substrate interface. All tests were designed to have a rapid heating time (10 min from room temperature to 800 °C) and cooling (10 min from 800 °C to near room temperature) rates to evaluate mainly the thermal shock resistance of the coated coupons instead of their oxidation resistance. In most cases, major failure is located in the coating/substrate interface, and thereby coating adhesive strength to the substrate can be evaluated by thermal cycling test (Ref 17). The ongoing test will be able to determine coating adhesion among specimens under this simulated high-temperature condition.

3.5 Erosion Resistance

The erosion resistance of the HVOF and LS-HVOF coatings were estimated at 25 and 300 °C, and the results are listed in Table 3. LS-HVOF coatings did not demonstrate a superior wear resistance in comparison to those of HVOF sprayed coating at both 25 and 300 °C, but did show a two or three times higher erosion rate. The microhardness HV (300 g) of the LS-HVOF coatings is on the average 375 HV (300 g), and for the HVOF coating it is 345 HV (300 g). It is obvious that the erosion rates are not directly related to coating hardness.

It is assumed that splat boundaries are the weakest location for coating cohesion. The small-grained microstructure in a LS-HVOF coating will not show any benefit in the erosion test if the impact force is high enough to pull out the splats. However, when the force by the impacting grit is not sufficient to pull out the splats at the boundaries, the coating fatigue will then become the dominant mechanism for material removal. Then, a fine-grained coating could demonstrate some advantages in erosion resistance over a coarse-grained coating. With this assumption, the low erosion resistance of LS-HVOF samples may be attributed to increased oxidation of the small alloy particles and the erosion test method. Due to the small diameter of the metallic particles, more oxides were probably produced on the surface of the particles during HVOF process. It is widely known that ceramics (e.g., oxides) will not have very good erosion resistance at a 90° impact angle. The conventional HVOF, with large metallic particles (less oxidation), was probably "more metallic" than the LS-HVOF coatings. Further tests are expected to clarify the possibility of increased oxidation in the LS-HVOF process and the effect of the impact angle on erosion rate. In addition, erosion tests need to be performed under conditions of similar service environment, using micrometer-sized particles/ashes, and similar particle velocity and pressure. As an exception, LS-HVOF No. 5 coating showed enhanced erosion resistance at higher temperature. The result implies that coating ductility (and potentially internal stress), which depends on grain structure and temperature, may be one of the determinant aspects responsible for its erosion behavior.

4. Conclusions

A new HVOF process has been developed to conduct spraying of small Inconel alloy 625 particles by utilizing a liquid carrier to deliver the fine particles in a suspension. The coatings formed by the process have several desirable aspects, including full density, uniform microstructure, and high bond strength. The main contributors to those improvements are better melting and higher velocity of the fine particles, revealed by process diagnostic analysis and metallographic observations. Coatings produced by conventional HVOF and the newly developed LS-HVOF processes were compared in terms of their mechanical properties, thermal shock resistance, and erosion resistance. Results verified that the fine-structured HVOF coatings have superior coating integrity, surface quality, adhesion, and ductility as compared with the coarse-structured HVOF coatings, although additional tests are required to further evaluate their performances in simulated service environment for fossil-fuel-fired boilers—one of the targeted applications. The preliminary erosion tests carried out at 90° impact angle indicated that the conventional HVOF coating was superior to the LS-HVOF coatings.

Acknowledgment

The authors would like to thank Paul Bryant, Inframat Corporation, for beneficial discussion on this work.

References

1. G.H. Joseph and P.E. Singer, *Combustion Fossil Power,* Rand McNally, 1991

2. D.B. Meadowcroft, High Temperature Corrosion Alloys and Coatings in Oil- and Coal-Fired Boilers, *Mater. Sci. Eng.,* 1987, **88,** p 313-320
3. K. Yamada, Y. Tomono, J. Morimoto, Y. Sasaki, and A. Ohmori, Hot Corrosion Behavior of Boiler Tube Materials in Refuse Incineration Environment, *Vac.,* 2002, **65,** p 533-540
4. V.H. Hidalgo, F.J.B. Varela, and E.F. Rico, Erosion Wear and Mechanical Properties of Plasma Sprayed Nickel- and Iron-Based Coatings Subjected to Service Conditions in Boilers, *Tribol. Int.,* 1997, **30**(9), p 641-649
5. G. Lai, Performance of Automatic GMAW Overlays for Waterwall Protection in Coal-Fired Boilers, *Metall. Eng.,* 2002, **4**(12), p 712-719
6. J.N. Dupont, J.R. Regina, and A.R. Marder, "Corrosion Behavior of Fe-Cr-Al Weld Overlay Coatings in High Temperature Oxidizing/Sulfidizing Environments," EPRI Conf. Mater. Corr. Experience in Fossil Power Plants, Electric Power Research Institute, 2003
7. J.R. Regina, J.N. Dupont, and A.R. Marder, High Temperature Behavior of Fe-Al Weld Overlayer Coatings for the Protection of Boiler in Low NOx Environments, 29th Proc. Int. Technical Conf., *Coal Utilization & Fuel System,* 2004, **1,** p 397-408
8. P.E. Chandler and M.B.C. Quigley, The Application of Plasma Sprayed Coatings for the Protection of Boiler Tubing, *Advances in Thermal Spray: 11th Proc. Int. Thermal Spray Conf.,* Pergamon, 1986, p 29-35
9. V. Higuera, F.J. Belzunce, A. Carriles, and S. Poveda, Influence of the Thermal Spray Procedure on the Properties of a Nickel-Chromium Coating, *J. Mater. Sci.,* 2002, **37**(3), p 649-654
10. K. Yamada, M. Koyama, T. Ohtsuka, M. Ohsawa, K. Tohyama, and K. Kakeda, Application of Thermal Spray Coating to Boiler Tubes in Refuse Incineration Plants, *Thermal Spraying: Current Status and Future Trends* (Kobe, Japan), May 22-26, 1995, Vol 1, A. Ohmori, Ed., ASM International, 1995, p 223-228
11. B.S. Sidhu, D. Puri, and S. Prakash, Characterizations of Plasma Sprayed and Laser Remelted NiCrAlY Bondcoats and Ni_3Al Coatings on Boiler Tube Steels, *Mater. Sci. Eng. A,* 2004, **368,** p 149-158
12. G.Y. Liang and T.T. Wong, Microstructure and Characterization of Laser Remelting of Plasma Sprayed Coating (Ni-Cr-B-Si) on Al-Si Alloy, *Surf. Coat. Technol.,* 1997, **89**(1-2), p 121-126
13. "Adhesion or Cohesive Strength of Flame-Sprayed Coatings," C633, *Annual Book of ASTM Standards,* ASTM
14. H.V. Higuera, F.J. Belzunce, and M.A. Carrilez, Characterization and High Temperature Behavior of Thermal Sprayed Coatings Used in Boilers, *Thermal Spray: Meeting the Challenges of the 21st Century* (Nice, France), May 25-29, 1998, Proc. 15th Int. Thermal Spray Conf., Vol 1, C. Coddet, Ed., 1998, p 617-621
15. F. Otsubo, H. Era, and K. Kishitake, Interface Reaction between Nickel-Base Self-Fluxing Alloy Coating and Steel Substrate, *J. Therm. Spray Technol.,* 2000, **9**(2), p 259-263
16. A. Tomiguchi, Y. Sochi, and Y. Matsubaray, Advantages of Induction Heat Treatment in the Application of Self-Fluxing Alloy to Boiler Tubes, *Thermal Spray: Meeting the Challenges of the 21st Century* (Nice, France), May 25-29, 1998, Proc. 15th Int. Thermal Spray Conf., Vol 1, C. Coddet, Ed., 1998, p 1061-1065
17. T. Sundararajan, S. Kuroda, F. Abe, and S. Sodeoka, Effect of Thermal Cycling on the Adhesive Strength of Ni-Cr Coatings, *Surf. Coat. Technol.,* 2005, **194**(2-3), p 290-299